ARTICLES

Formation of anion-vacancy clusters and nanocavities in thermochemically reduced MgO single crystals

M. A. Monge, A. I. Popov,* C. Ballesteros, and R. González

Departamento de Física, Escuela Politécnica Superior, Universidad Carlos III, Avda. Universidad 30, 28911 Leganés, Madrid, Spain

Y. Chen

Division of Materials Sciences, Department of Energy, Germantown, Maryland 20874-1290

E. A. Kotomin*

Max-Planck Institut für Festkörperforschung, Heisenberstrasse 1, Stuttgart 70569, Germany

(Received 2 February 2000)

An MgO crystal was thermochemically reduced (TCR) under extreme reducing conditions such that the concentration of anion vacancies (F centers) was exceptionally large, 6×10^{18} cm^{-3}. Optical absorption measurements demonstrate that in addition to F centers absorbing at 250 nm, anion-vacancy clusters absorbing at 355, 406, 440, 480, and 975 nm were observed. Upon thermal annealing in a reducing atmosphere, a broad extinction band at 345 nm with a full width at half maximum (FWHM) of 1.25 eV emerged. With further heat treatment the peak wavelength shifted toward 370 nm and the FWHM varied between 1.25 and 2.25 eV. Transmission electron microscopy (TEM) showed that concomitantly there exist rectangular defects with typical dimensions of 3 nm. Microdiffraction, x-ray microanalysis, and high-resolution electron microscopy, in conjunction with Mie theory, indicate that these rectangular defects are nanocavities with their walls plated with magnesium. Therefore, both oxygen vacancies and magnesium-rich regions have been observed in a thermochemically reduced MgO crystal.

I. INTRODUCTION

Point defects in the form of oxygen vacancies in MgO crystals can be produced by two methods: irradiation with energetic particles, such as neutrons, electrons, or ions,[1–8] and thermochemical reduction (TCR) performed under very severe environmental conditions, resulting in stoichiometric imbalance of the oxygen sublattice.[5,9–11] These defects can be well characterized spectroscopically by their optical and magnetic properties.

In general, irradiation with energetic particles results in vacancies and interstitials in both the anion and cation sublattice.[12] Interstitials are difficult to detect; therefore most studies involve vacancies. These vacancies are usually not stable at temperatures not much above room temperature, because they recombine with the more mobile interstitials.[5] If the irradiating particle is sufficiently energetic, higher-order vacancies involving both sublattices can occur.[1–8] In TCR crystals there are no interstitials and the vacancies can therefore survive at much higher temperatures.[5] By virtue of the mass-action law, the vacancies created nonstoichiometrically are mostly anion vacancies and their clusters. However, if impurities are present, TCR can result in the formation of precipitates containing the impurities.[13–22]

The irradiation of undoped MgO crystals by energetic neutrons ($E > 0.1$ MeV) produces several optically detectable defects: (1) single-charged anion vacancies (the one-electron F^+ center), which absorbs at 252 nm (4.92 eV),[3,6] (2) neutral anion divacancies or F_2 centers, which absorb at 355 and 975 nm (3.49 and 1.27 eV, respectively),[1,2,5,7] and (3) an unidentified aggregate defect, which absorbs at 573 nm (2.16 eV).[3–5,7,8] Energetic particles displace magnesium ions, but the magnesium interstitials are sufficiently mobile near room temperature that they quickly recombine with magnesium vacancies. In TCR crystals, the anion vacancies prefer to be in the neutral F state (oxygen vacancies each with two electrons), unless stimulated by photons or charge particles. Upon a moderate heat treatment, > 450 K, any F^+ centers revert back exclusively to F centers.[9] F centers absorb at 247 nm (5.01 eV), essentially at the same energy as the F^+ centers.[3]

If TCR results in isolated anion vacancies scattered randomly, the probability of forming aggregate centers in TCR crystals will depend nonlinearly on the concentration of single anion vacancies. The probability for F_2 is quadratic in the concentration of the F centers.[12] Thus, the absorption band of the F_2 center can only be resolved in crystals containing a very high concentration of F centers.[5] Uniaxial stress and polarized luminescence measurements at low temperature in TCR MgO crystals suggested that the luminescence bands at 375 and 441 nm, attributed to F_2 and F_2^{2+} dimer centers, respectively, have excitation peaks at 355 and 322 nm, respectively.[23–25] Kinetic arguments suggest that F_3 centers and higher-order defects are formed at much lower rates than F_2 centers.[12,26]

TCR implies (a) a deficiency of oxygen, resulting in oxy-

gen vacancies in the neutral *F* state (this has been well substantiated in the literature) and (b) an excess of magnesium. This has not been observed. In the present study, we provide evidence that there are regions rich in magnesium.

II. EXPERIMENTAL PROCEDURES

The MgO crystals used were grown at the Oak Ridge National Laboratory using the arc fusion technique.[27] The starting material was MgO powder from the Kanto Chemical Company, Japan. TCR was performed in a sealed tantalum chamber at ≈ 2400 K and greater than 7 atmospheres of magnesium vapor, followed by rapid cooling. This process produces anion (oxygen) vacancies, due to a stoichiometric excess of cations. A crystal with a very high concentration of *F* centers ($\approx 6 \times 10^{18}$ cm^{-3}) was cleaved into several samples. Subsequent reducing heat treatments of the TCR samples were made inside an enclosed graphite chamber inserted in a horizontal furnace with flowing high-purity nitrogen gas.

Optical absorption measurements in the uv-visible-ir wavelengths were made with a Perkin-Elmer Lambda 19 spectrometer. Infrared absorption data were taken with a Perkin-Elmer 2000 FT-IR spectrometer. Irradiations with uv light were made either with a Mineralight lamp (model UVGL 25) or a 500-W Xe(Hg) lamp in conjunction with a 7200 Oriel monochromator. Specimens for transmission electron microscope (TEM) studies were prepared by mechanical grinding, dimpling, and argon ion-milling with an acceleration voltage of 5 kV and an incident angle of 10°. TEM, x-ray microanalysis, and electron diffraction studies were carried out in a Philips CM200 field-emission analytical electron microscope operated at 200 kV and equipped with a beryllium specimen holder.

III. RESULTS AND DISCUSSION

A. Optical absorption and extinction measurements

Defects resulting from TCR of MgO crystals at high temperature are primarily isolated *F* centers that absorb light at about 250 nm. If hydrogen impurities are present in the crystal, they can be trapped at these vacancies, forming H$^-$ ions that absorb in the far-infrared region at about 1000 cm^{-1}.[10] The more hydrogen the crystals contain, the more H$^-$ ions are formed. Thus the balance between the anion vacancy and the H$^-$ ion concentrations depends on the concentration of hydrogen in the crystal. In order to maximize the anion vacancy content and minimize the H$^-$ concentration, a clear crystal with a low hydrogen concentration was thermochemically reduced. From the experimentally derived relation[11]

$$n(\text{H}^-) = 2.7 \times 10^{17} \alpha(1053), \qquad (1)$$

where $\alpha(1053)$ is the absorption coefficient of the 1053 cm^{-1} peak, the resulting H$^-$ concentration was estimated to be $\leqslant 10^{16}$ cm^{-3}.

Figure 1 [spectrum (a)] is the optical absorption spectrum of the crystal after TCR. The most prominent feature is the very high anion vacancy absorption at 250 nm. Using the experimentally derived relation[28]

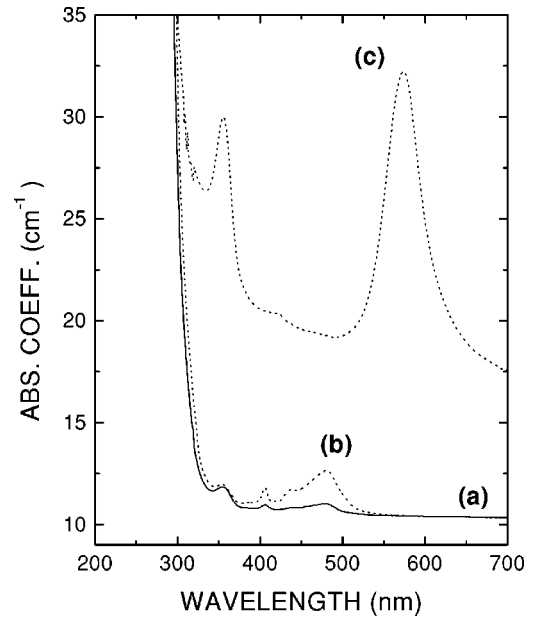$$n(F) = 5 \times 10^{15} \alpha(F), \qquad (2)$$

FIG. 1. Optical absorption spectra of (a) MgO crystal after TCR and (b) after subsequent uv irradiation for 15 min; (c) neutron-irradiated MgO crystal up to a dose of 6.9 $\times 10^{18}$ neutrons cm^{-2} s^{-1}.

where $n(F)$ denotes the concentration of anion vacancies and $\alpha(F)$ is the absorption coefficient of the 250-nm band, the concentration of isolated *F* centers was estimated to be $\approx 6 \times 10^{18}$ cm^{-3}. In addition, other bands at about 355 nm (3.49 eV), 406 nm (3.05 eV), 440 nm (2.82 eV), 480 nm (2.58 eV), and 975 nm (1.27 eV) are also present (the 975-nm band is not shown in Fig. 1). These bands became more pronounced after uv excitation for 15 min [spectrum (a) in Fig. 1]. Spectrum (b) reverted to spectrum (a) when the sample was heated at 773 K. For comparison, the spectrum of a neutron-irradiated crystal with a similar concentration of anion vacancies (mostly F^+ centers) is also shown [trace (c)]. Only the bands at 250, 355, and 975 nm appear in both TCR and neutron-irradiated crystals. The bands at 335 and 975 nm are different transitions of the F_2 centers.[1,2,5,7] Also, the excitation spectrum for the luminescence at 375 nm in TCR crystals peaks at 357 nm and was associated with these centers,[24] which agrees very well with our absorption measurements. Table I summarizes the optical absorption bands in both TCR and neutron-irradiated crystals.

Next, we will discuss the effects of thermal anneals of this sample in a reducing atmosphere. It was isochronally annealed for 5 min at increasing temperatures of 50-K intervals starting at 1173 K. Figure 2 shows the absorption spectra at several selected temperatures. After the annealing at about 1373 K, the sample started to develop a brown coloration due to a broad extinction band covering most of the visible region and centered at about 345 nm (3.59 eV). As the temperature was raised this band shifted in wavelength and became more intense. The maximum intensity occured after annealing at 1673 K [Fig. 2(a)]. Meanwhile the *F* band decreased. Annealing treatments at $T > 1673$ K decreased the intensity of the extinction band. At 1873 K the band disappeared and the sample became transparent [Fig. 2(b)]; the *F* band also annealed out. The isochronal annealing data of the

TABLE I. Optical absorption bands in thermochemically reduced and neutron-irradiated MgO crystals.

				Wavelength (nm)				
TCR	247 (5.01 eV)	232 (3.85 eV)	355 (3.49 eV)	406 (3.05 eV)	440 (2.82 eV)	480 (2.58 eV)		975 (1.27 eV)
Neutron-irradiated		252 (4.92 eV)	355 (3.49 eV)				573 (2.16 eV)	975 (1.27 eV)
Assigment	F	F^+	F_2^{2+}	F_2	?	?	?	F_2

250 and ''345'' nm bands are plotted in Fig. 3. The F band decreases with annealing temperature whereas the ''345''-nm band increases.

Both the position and the full width at the half maximum (FWHM) of the ''345''-nm band changes with the thermal treatment (Fig. 4). The 345-nm peak shifted to 370 nm (top). The FWHM varied from 1.25 to 2.25 eV (bottom). These two behaviors suggest that this band is due to Mie scattering from metallic colloids.[13] Indeed, a similar extinction band with its peak at 340 nm and a FWHM of 1.2 eV was observed[29] in MgO implanted with Mg^{2+} ions after thermal annealing at 1173 K. These TEM observations showed that this band was due to magnesium precipitates with an average size of ≈ 77 Å.

B. Mie theory

According to Mie theory (see Ref. 13 and references therein), the extinction coefficient due to a dilute concentration N of spherical particles of radius R and volume V embedded in a dielectric medium with a homogeneous distribution is given by

$$\gamma = \frac{6\pi NV}{\lambda'} \mathrm{Im} \sum_{v=1}^{\infty} (-1)^v \frac{a_v - p_v}{2\alpha^3},\qquad (3)$$

where λ' is the wavelength of the light in the matrix and $\alpha = 2\pi(R/\lambda')$. The quantities a and p are the electric and magnetic multipoles of order v, which are functions of the colloid radii and of the dielectric constant of both the particles and the matrix.

For small colloids ($R < 10$ nm), using only the first term in Eq. (3), the extinction maximum occurs at a wavelength λ given by

$$\lambda = \frac{2\pi c}{\omega_p}(\epsilon_0 + 2m_0^2)^{1/2}.\qquad (4)$$

Here c is the vacuum speed of light, ω_p the plasma frequency of the metal, $\epsilon_0 \approx 1$ the static dielectric constant of the metal, and $m_0^2 = 1.774$ the real part of the dielectric constant of the MgO matrix.

Equation (4) indicates that the position of the maximum is independent of the colloid radius. Assuming that the precipitates are made of metallic magnesium, $\omega_p = 1.63 \times 10^{16} \mathrm{s}^{-1}$,[30] the predicted wavelength of the peak of the extinction band is 320 nm, in reasonable agreement with the experimental findings of about 345 nm. The discrepancy between the theoretical and the experimental values can prob-
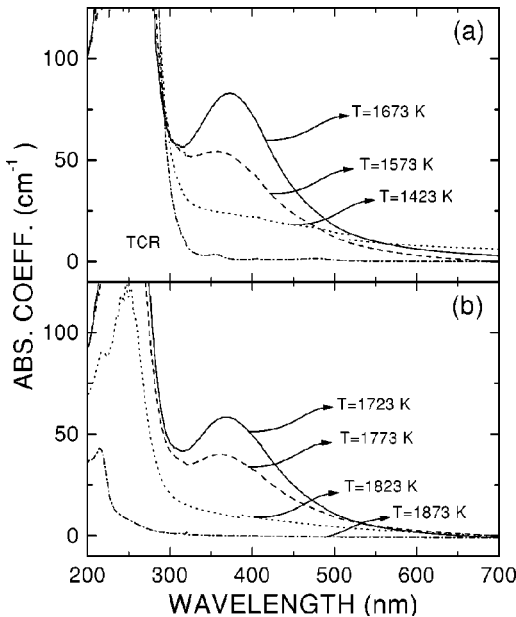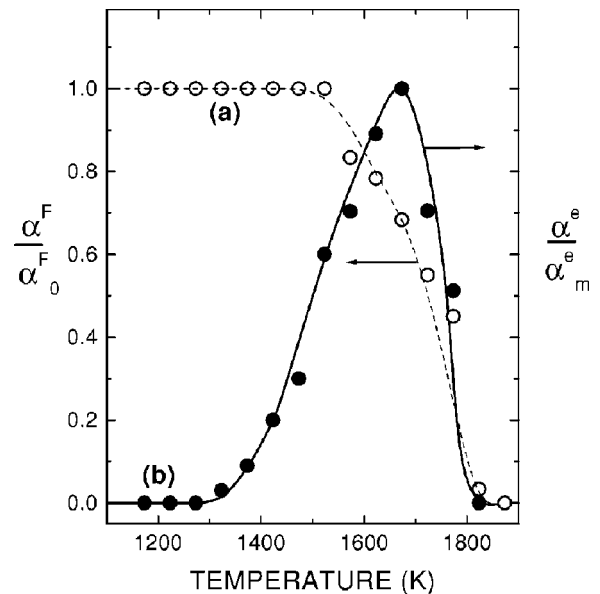

FIG. 2. Optical absorption spectra of a thermochemically reduced MgO crystal isochronally annealed in a reducing atmosphere. (a) formation of the 345–370-nm band, (b) destruction of the 345–370-nm band.

FIG. 3. Normalized concentration of (a) F centers, and (b) 345–370-nm extinction band vs isochronal annealing temperature. It is noted that the initial F band was so large that the errors involved in determining the F-center concentration are correspondingly large.
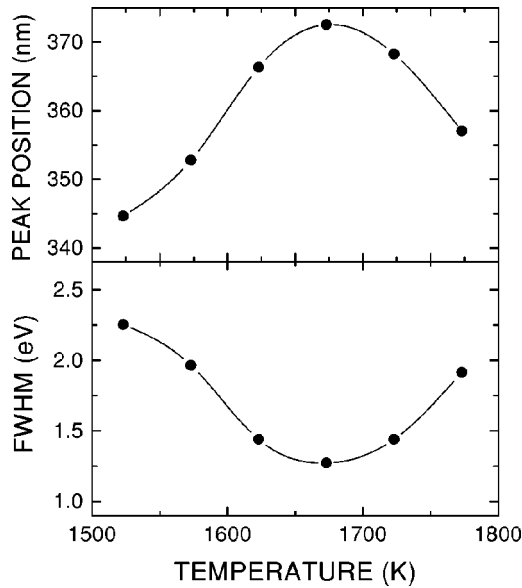
FIG. 4. Peak position and FWHM of the 345-nm band band vs isochronal annealing temperature. At temperatures below 1523 K, the deconvolution of the bands was not very accurate; thus, the corresponding values for the peak position and the FWHM were not plotted.

ably be partially solved by taking into account the probability of the electrons being outside the colloid. Then Eq. (4) becomes[31]

$$\lambda = (1 - 3P)^{-1/2} \frac{2\pi c}{\omega_p} (\epsilon_0 + 2m_0^2)^{1/2}, \qquad (5)$$

where P represents the probability for each electron of being outside the colloid. The prefactor $(1 - 3P)^{-1/2}$ is higher than unity, which implies that the new predicted position of the band, λ, occurs at longer wavelengths, as was experimentally found.

In order to calculate extinction bands as a function of size, it is necessary[13] to use higher-order terms in the Mie equation (3). Assuming that the magnesium colloids are small compared with the mean free path of the electrons in the bulk, the FWHM of the extinction band, ΔE, is proportional to v_F / R, where $v_F = 1.58 \times 10^{18} \, \text{cm}^{-3}$ is the Fermi velocity of electrons and R the mean radius of the precipitate.[13] Using the experimental values for ΔE, we estimate the colloid mean radius to range from 2.8 to 5.2 nm. Figure 5 shows the colloid radius as a function of the annealing temperature. The largest value of 5.2 nm corresponds to colloids after the annealing at 1673 K. The optically suggested precipitates are to be confirmed by TEM observations.

C. Transmission electron microscopy

Electron microscopy observations were made in the same TCR sample after annealing at 1673 K in a reducing atmosphere. A brown coloration due to the extinction band, which had shifted from 345 to 370 nm [see Figs. 2(a) and 4(a)], was observed. The characteristic bright-field images are shown in Figs. 6 and 7. Areas with a high concentration of dislocations (Fig. 6) were separated by regions in which only small rectangular features are observed (Fig. 7). In order to investigate
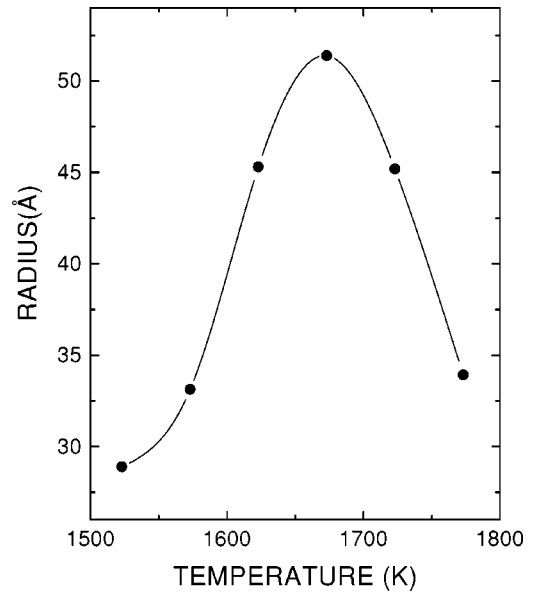

FIG. 5. Calculated colloid radius vs isochronal annealing temperature.

the structure and composition of these rectangular defects, microdiffraction patterns and x-ray microanalysis spectra were obtained both inside and outside the rectangle defects. No appreciable differences were observed. These results indicate that the structure and the composition are those of a perfect MgO structure in both cases.

To explore further the nature of these rectangular defects, high-resolution electron microscopy (HREM) was used. Figure 8 shows a high-resolution image along the $\langle 001 \rangle$ direction. The atomic plane structure within the region containing rectangle defects is the same as that everywhere else. We conclude that the rectangular defects are nanocavities with $\{100\}$ facets and an average size of about 3 nm. Association of cavities with facets parallel to the $\{100\}$ planes was also observed.

The TEM results clearly showed that the rectangular defects were not due to a second phase, but rather to nanosize
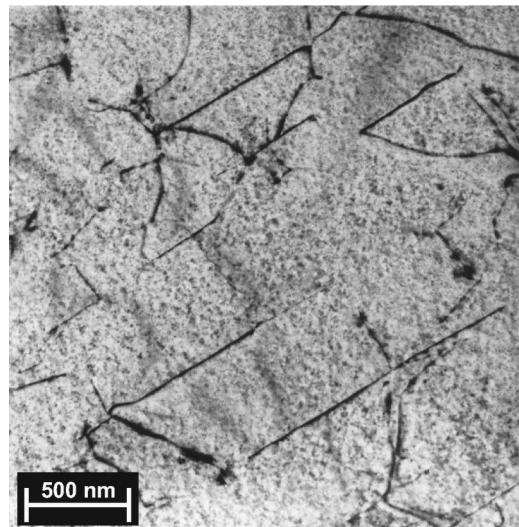

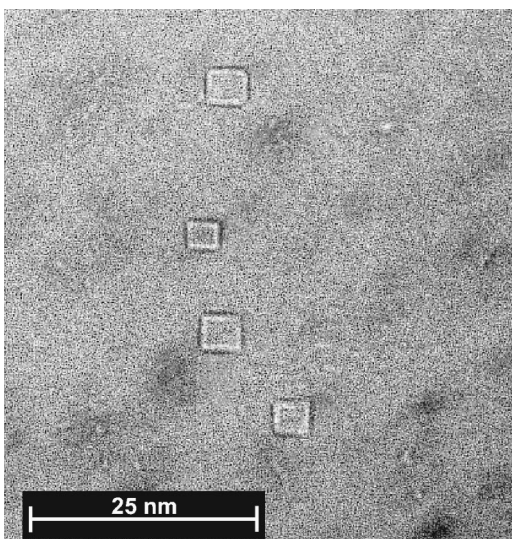FIG. 6. Bright-field electron micrograph showing dislocations in the TCR sample after annealing at 1673 K.

FIG. 7. Bright-field electron micrograph showing rectangular defects in the TCR sample after annealing at 1673 K.

FIG. 8. High-resolution electron micrograph of the TCR sample after annealing at 1673 K, showing an area containing nanocavities.

cavities. The presence of an optical extinction band associated with these cavities suggests that the boundary region between a nanocavity and the MgO matrix must be rich in magnesium since the characteristics of the extinction band agree with those predicted by the Mie theory for magnesium colloids. It should be noted that Mie theory can also be applied to colloids with an empty core.[32] In conclusion, the defects responsible for the 370-nm extinction band are probably nanocavities surrounded by a thin magnesium-rich layer.

Unfortunately, additional evidence for the composition of the defects observed here it is not easy to obtain. The concentration of nanocavities, estimated to be 10^{11} cm^{-3}, is too low to permit meaningful x-ray diffraction studies. Likewise, simulations of high-resolution images with and without Mg inside the cavities are not reliable since the images were obtained in thick areas of the specimen.

In the bigger picture the thermochemical reduction process can have the following consequences: (a) a deficiency of oxygen ions, resulting in oxygen vacancies and/or clusters of oxygen vacancies, and (b) an excess of magnesium, which plates the walls of the nanocavities, as shown in the present study.

IV. SUMMARY AND CONCLUSIONS

A nominally pure MgO crystal was thermochemically reduced (TCR) under extremely stringent conditions such that the concentration of anion vacancies (F centers) was extraordinarily large, 6×10^{18} cm^{-3}. In addition to the intense absorption of the F centers at 250 nm, other much weaker bands at 355, 406, 440, 480, and 975 nm were observed. By nature of the strong thermochemical reduction, these weak bands are likely due to clusters of anion vacancies. Indeed,
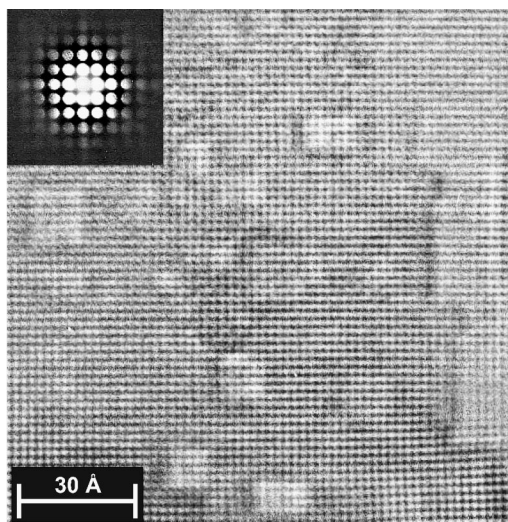
the bands at 355 and 975 nm had been identified as due to different transitions within F_2 centers.[1,2,5,7]

After isochronal anneals in a reducing atmosphere above 1373 K, the sample exhibited a brown coloration due to the formation of an extinction band at about 345 nm. Both the peak-extinction wavelength and the FWHM of this band changed with annealing temperature. The peak wavelength shifted from 345 to 370 nm. The maximum extinction intensity occurred at 1673 K. The FWHM varied between 1.25 and 2.25 eV. After the anneal at 1873 K, the sample became transparent, indicating that the defects responsible for the brown coloration were annealed out.

TEM revealed rectangular defects with typical dimensions of 3 nm. Microdiffraction patterns, x-ray microanalysis, and high-resolution electron microscopy, in conjunction with the Mie theory, indicate that these rectangular defects are nanocavities with their walls plated with magnesium.

The two essential implications of thermochemical reduction in high-pressure magnesium vapor at high temperatures have been observed: (a) a deficiency of oxygen vacancies and their clusters, and (b) an excess of magnesium, which plates the walls of the nanocavities.

*Permanent address: Institute of Solid State Physics, University of Latvia, 8 Kengaraga, Riga, LV-1063, Latvia.

[1] I.K. Ludlow and W.A. Runciman, Proc. Phys. Soc. London **86**, 1081 (1965).

[2] B. Henderson and J.E. Wertz, Adv. Phys. **17**, 749 (1968).

[3] Y. Chen, J.M. Kolopus, and W.A. Sibley, Phys. Rev. **186**, 865 (1969).

[4] Y. Chen and W.A. Sibley, Philos. Mag. A **20**, 217 (1969).

[5] Y. Chen, R.T. Williams, and W.A. Sibley, Phys. Rev. **182**, 960 (1969).

[6] L.A. Kappers, R.L. Kroes, and E.B. Hensley, Phys. Rev. B **1**, 4151 (1970).

[7] B. Henderson, CRC Crit. Rev. Solid State Mater. Sci. **9**, 1 (1980).

[8] R. González, Y. Chen, R.M. Sebek, G.P. Williams, Jr., R.T. Williams, and W. Gellermann, Phys. Rev. B **43**, 5228 (1991).

[9] L.A. Kappers and E.B. Hensley, Phys. Rev. B **6**, 2475 (1972).

[10] R. González, Y. Chen, and M. Mostoller, Phys. Rev. B **24**, 6862 (1981).

[11] Y. Chen, R. González, O.E. Schow, and G.P. Summers, Phys. Rev. B **27**, 1276 (1983).

[12] E. Sonder and W.A. Sibley, *Point Defects in Solids*, edited by J. H. Crawford, Jr. and L. M. Slifkin (Plenum, New York, 1972), Vol. 1, p. 201.

[13] A.E. Hughes and S.C. Jain, Adv. Phys. **28**, 717 (1979).

[14] J. Narayan, Y. Chen, and R.M. Moon, Phys. Rev. Lett. **46**, 1491 (1981).

[15] J. Narayan, Y. Chen, R.M. Moon, and R.N. Carpenter, Philos. Mag. A **49**, 287 (1984).

[16] R.M. Bunch, W.P. Unruh, and M.V. Iverson, J. Appl. Phys. **58**, 1474 (1974).

[17] C. Ballesteros, R. González, and Y. Chen, Phys. Rev. B **37**, 8008 (1988).

[18] C. Ballesteros, R. González, S.J. Pennycook, and Y. Chen, Phys. Rev. B **38**, 4231 (1988).

[19] C. Ballesteros, L.S. Cain, S.J. Pennycook, R. González, and Y. Chen, Philos. Mag. A **59**, 907 (1989).

[20] C. Ballesteros, R. González, Y. Chen, and M.R. Kokta, Phys. Rev. B **47**, 2460 (1993).

[21] C. Ballesteros, Yi Chen, Y. Chen, R. González, M.R. Kokta, and X.F. Zong, Philos. Mag. A **76**, 357 (1997).

[22] B. Savoini, C. Ballesteros, J.E. Muñoz Santiuste, R. González, and Y. Chen, Phys. Rev. B **57**, 13 439 (1998).

[23] M. Glasbeek, R. Sitters, and B. Henderson, J. Phys. C **13**, L1021 (1980).

[24] D.O. O'Connel, B. Henderson, and J.M. Bolton, Solid State Commun. **38**, 283 (1981).

[25] J.M. Bolton, B. Henderson, and D.O. O'Connel, Solid State Commun. **38**, 287 (1981).

[26] F. Agulló-López, C.R.A. Catlow, and P.D. Townsend, *Point Defects in Materials* (Academic Press, New York, 1988), Chaps. 5 and 6.

[27] M.M. Abraham, C.T. Butler, and Y. Chen, J. Chem. Phys. **55**, 372 (1971).

[28] W.A. Sibley and Y. Chen, Phys. Rev. **160**, 712 (1967).

[29] M. Treilleux, P. Thevenard, G. Chassagne, and M. Guermazi, Surf. Sci. **106**, 165 (1981).

[30] P.M.Th.M. van Attekum, and J.M. Trooster, Phys. Rev. B **20**, 2335 (1979).

[31] J.R. Weerkamp, J.C. Groote, J. Seinen, and H.W. den Hartog, Phys. Rev. B **50**, 9781 (1994).

[32] K. Schwartz and J. Ekmanis, *Dielectric Materials: Radiation-Induced Processes in Insulating Solids* (Zinatne, Riga, 1989) (in Russian).